Efficient and precise? – Evaluation of a mobile mapping system in the context of road surface monitoring

Markus WAGNER[1,*], **Berit JOST**[1], **Lasse KLINGBEIL**[1], and **Heiner KUHLMANN**[1]

[1] *Institute of Geodesy and Geoinformation, University of Bonn, Germany, (wagner@igg.uni-bonn.de)*

[*] *corresponding author*

Abstract

Deformations of the road surface due to high traffic load shorten the life span of the road and negatively influence the safety of the traffic participants. Usually, special sensor systems are used to monitor road conditions, which are expensive and only built for one particular application. Mobile mapping systems, however, capture their close environment including the road surface. With the processed point cloud, multiple parameters can be derived. The major drawback of these systems is, that the uncertainty of the measured points and accordingly of the derived parameters is unknown and hard to derive. However, the uncertainty of the derived parameters is crucial for the interpretation. Within this study, we empirically evaluate the uncertainty of a mobile mapping system in the context of road surface monitoring. The considered parameters are the road cross fall and the rut depth. We repeatedly measure the road surface from both driving directions and extract the mentioned parameters for each pass at the same location from the point cloud data. Two data sets with different environmental conditions are considered, to evaluate the influence of the environmental conditions. This study demonstrates that the road cross fall is sensitive to remaining errors in the system calibration. The rut depth only depends on the uncertainty of the used profile laser scanner and on the used algorithm, especially the detection of the support points.

Keywords: deformation monitoring, mobile mapping, uncertainty evaluation, road parameters

1 Introduction

The road network is one key infrastructure for the society and economy of a country. In 2023 over 70 percent of the freight transport was performed by trucks in Germany[1]. Additionally, 58 percent of trips with at least one overnight stay from german citizens were made by car. The high demand for road infrastructure leads to a faster deterioration of the road surface quality and consequently to a faster need for rehabilitation. Bad road conditions can negatively influence the driver's safety and has also a bad influence on the traffic flow and fuel costs. In 2021/22 over 7000 kilometers of highways are ranked as in need of rehabilitation by the Federal Ministry of Transport in Germany.

The road quality is classified by considering different quality features like the skid resistance or the evenness, which should be regularly inspected by hand or with kinematic multi-sensor systems. These systems are built to measure specific road quality features, like the evenness of the cross-profile and along the road axis (FGSV, 2009). The major advantage of the kinematic approach is, that the measurement can be performed much faster and without traffic interference.

Mobile mapping systems (MMS) are capable of measuring the geometry of the road surface as well as the near surroundings of the roads and are used by surveying companies for different mapping applications. Recent publications show the use of such systems for road surfacing monitoring (Ma et al., 2024; Miraliakbari et al., 2014), which may help to increase the number of monitored roads per year. The main disadvantage of MMS is the lack of knowledge regarding uncertainty, which is key information for the correct interpretation, especially for monitoring applications. Consequently, the uncertainty of the considered parameter like the evenness has to be known and has to be small enough to be able to interpret the resulting values. To our knowledge, the evaluation of these parameter uncertainties is con-

[1] www.statista.com

ducted by only comparing the results to ground truth data without analyzing the potential influencing factors. This leads to the problem, that the resulting uncertainty cannot be referred to certain error sources within the processing chain.
In this paper, we present an empirical approach to evaluate the uncertainty of a mobile mapping system in the context of the extraction of two road quality parameters: the road cross fall describing the inclination and the rut depth describing the evenness of the road cross section. We therefore use the road surface itself and derive the parameters at different positions multiple times by performing repeated measurements. To evaluate the uncertainty of both parameters properly, four key questions are tackled in this work, which might influence the uncertainty and which can change considering the used system and the environmental conditions:

- **How do the environmental conditions influence the uncertainty of the considered parameters?** Bad GNSS conditions indicated by a small number of visible satellites or high Positional Dilution of Precision (PDOP) values (Teunissen and Montenbruck, 2017) lead to inaccurate pose estimation. The pose information is one of the largest influencing factors on the MMS point cloud.
- **How does the system calibration influence the uncertainty of the considered parameters?** The relative position and orientation of the scanner coordinate system and the body frame, where the trajectory information is given, should be known to achieve an accurate point cloud. Errors in the boresight angles for example lead to a constant tilt of the point cloud relative to the position of the system.
- **How do the scanner properties influence the uncertainty of the considered parameters?** The point spacing and the measurement noise vary depending on the used scanner, which influences the description of the road surface.
- **How does the surface representation influence the uncertainty of the derived parameters?** Different surface representations may provide more precise rut depth estimation since they can deal better with noisy and sparse data.

The four questions will be tackled as follows: In section 2 the two considered parameters are explained and the considered data sets and the used system are presented. Additionally, the extraction and evaluation procedure of the considered parameters are explained. In section 3 the results from both data sets are shown and interpreted. A summary is given in section 4.

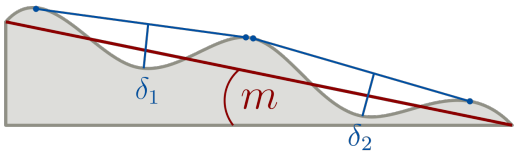

Figure 1. Cross section of one lane of the road surface and the considered parameters.

2 Materials and methods

Figure 1 shows a cross section of one lane of the road including the considered parameters, which are described in the following.

2.1 Road cross fall

The cross fall m describes the inclination of the cross section of the road surface, which ensures proper water drainage (see Figure 1). Furthermore, the road has to be inclined depending on the permitted velocity and the curvature, so centrifugal forces will not push the car outwards. Consequently, the magnitude of this value varies depending on the shape of the road section and is chosen during the planing process. For the determination of the road cross fall, GNSS measurements using two antennas can be used (Baffour, 2002). The height difference between both antennas and the knowledge about the baseline between them are used to compute the desired inclination. Tsai et al. (2013) uses a MMS point cloud to determine the cross fall at predefined regions along the road by fitting a regression line into the cross section of the road. Shams et al. (2018) computes the height differences and the distances between road markings in the cross section to determine the cross fall. In both works, the authors compare the results with digital level measurements. Both analyze the uncertainty on different data sets but they did not analyze the impact of the scanner properties on the results.

2.2 Rut depth

The rut depth δ describes the evenness of the road's cross section and is defined by the largest dimension between the rut bottom and a reference line, which is described by a 2 m rod (FGSV, 2009). In Figure 1 the rod is visualized by the blue lines for each of the two ruts on one lane. Rutting increases the danger of hydroplaning (Fwa et al., 2012), since water accumulates in the ruts and cannot run off properly and this negatively influences the driver's safety. For the determination of the rut depth using MMS, multiple approaches exist. In Ma et al. (2024), the points lying on the road profile are first filtered with a Vandrak filter, and the supporting points for the imaginary 2 m rod are found by computing the convex hull of the filtered points. They also changed the smoothing factor of the filter and analyzed its impact on the computed results. Other approaches fit polynomials into the cross section (Miraliakbari et al., 2014) and perform a feature matching to detect the location of the ruts. In Liu et al. (2022), the scanned road surface is converted into an elevation feature matching, and the ruts are detected using image processing algorithms. Some of the mentioned works also evaluate their approaches against ground truth data from e.g. terrestrial laser scans. Besides the evaluation for different surface representations or smoothing factors, the analysis regarding the other influencing factors was not performed to our knowledge.

2.3 Data collection

In this part, the MMS and the captured data sets are presented.

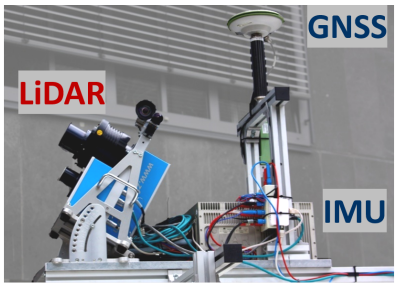

Figure 2. Used MMS. left: Z+F Profiler 9012A profile laser scanner; right: iMAR iNAV-FJI-LSURV IMU and RTK GNSS antenna

2.3.1 Measurement System

The mobile mapping system used in this work is shown in Figure 2. It consists of an inertial navigation system iMAR iNAV-FJI-LSURV (https://www.imar-navigation.de/en/) with fiber optic gyroscopes, servo accelerometers and RTK-GNSS (Real Time Kinematic) for the navigation. The trajectory estimation is performed in the software Waypoint Inertial Explorer 9.00 (NovAtel Inc, 2024). We use a virtual reference station computed by SAPOS NRW for the considered data sets in this work. The coordinate of the reference station is chosen in the center of the test environment, such that the maximum baseline is below 2 kilometers in both cases. For the mapping task, a 2D laser scanner Z+F Profiler 9012A is mounted on the system (Zoller & Fröhlich GmbH, 2020). The precision of the range measurement is specified as $0.2 - 0.5$ millimeters at a distance of 10 meters depending on the reflection properties of the measured surface. The chosen profile rate is 200 Hz and the scan rate is set to 1016 kHz for both data sets considered in this study. Considering the height of the used van, the point spacing κ_0 on the road surface is approximately 2.5 mm across the driving direction. The system calibration is done by a plane-based approach described in Heinz et al. (2020) in 2019. The authors showed, that the uncertainty of the lever arm is below 0.5 mm and below 0.002 deg of the boresight angles.

2.3.2 Country road data set

The first data set was captured on a country road near Cologne, Germany in winter 2023. Figure 3a shows the considered road part. The two-lane road part is around 3 km long and leads through a forest, so GNSS conditions are expected to be bad. The PDOP value is larger than 3.0 for the whole road part in the captured data set. The trees near the road occlude the sky, so that the GNSS signals are blocked or disturbed. The measurement starts at the northern town "Bensberg" and after driving over the reference road part, the system turns to the southern town "Forsbach" and drives back to "Bensberg". This procedure was performed five times so that the road surface was measured ten times.

2.3.3 Urban data set

The second data set was captured at the university campus "Poppelsdorf" in Bonn, Germany in

(a) Country road data set

(b) Urban data set

Figure 3. Overview of both data sets

the summer of 2024. Figure 3b shows the considered road parts. For the computation of the road quality parameters, only the blue highlighted road parts are considered. In the area around the "Meckenheimer Allee", the mean PDOP value is higher than 10, whereas, on the other "Endenicher Allee", the average value is around 2.9. The measurement starts at the parking lot southwest of the "Nussallee" (red dot). After turning in the "Nussallee", the system heads north-west and drives the whole track clockwise, turns at the parking lot, and drives then counter-clockwise. This procedure is performed five times so that the road surface is captured ten times in total.

2.4 Extraction of the road quality parameters

Since we want to analyze the impact of the environmental conditions on the cross fall and the rut depth, we need to compute them at different locations in the data sets. Therefore we define a regular grid

$$\mathscr{P} = \{\mathbf{X}^{(1)}_{grid}, \mathbf{X}^{(2)}_{grid}, \cdots \mathbf{X}^{(i)}_{grid}, \cdots \mathbf{X}^{(n)}_{grid}\} \qquad (1)$$

with a constant spacing 1 m along the given road axis, where both parameters are estimated. Both the grid points $\mathbf{X}^{(i)}_{grid}$ and the measured points in the point cloud are transformed to ETRS89/UTM coordinates with ellipsoidal height information as the z-component. For every grid point $\mathbf{X}^{(i)}_{grid}$, we extract the neighboring measured points $\mathbf{X}^{(i)}_{in}$ which are within a radius of $r = 10$ m. With this, we filter out unimportant points and decrease the memory consumption. Next, we transform the points $\mathbf{X}^{(i)}_{in}$, such

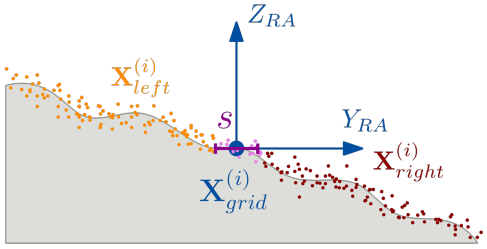

Figure 4. Extraction of the points lying on different lanes of the road's cross section

that the x-axis of the resulting coordinate system is parallel to the road axis defined by the generated grid $\mathscr{P}$. As a result, we receive the transformed points $\mathbf{X}^{(i)}_{RA}$, where the x-axis points along the road axis and the y-axis are parallel to the cross section of the road (see Figure 4). The origin of the coordinate system is the grid point $\mathbf{X}^{(i)}_{grid}$. We then filter out all points whose x-coordinate lies outside a certain interval with a width of $\varepsilon = 0.3$ m, since both parameters may vary along the road

$$\mathbf{X}^{(i)}_{buf} = \mathbf{X}^{(i)}_{RA}\left(|\mathbf{x}^{(i)}_{RA}| < \varepsilon\right). \qquad (2)$$

After that, we need to find the borders y_l and y_r of the road surface to filter out points that do not represent the road surface. This is done by analyzing the gradient of the z-component along the cross profile, to identify for instance curbs. But there are also other methods to extract the road border in point cloud data (Zhou et al., 2014).
Furthermore, we split the points into a left and right part based on the y-coordinate, because both road quality parameters are estimated for each lane sepa-

rately:

$$\mathbf{X}_{left}^{(i)} = \mathbf{X}_{buf}^{(i)} \left(\mathbf{y}_{buf}^{(i)} > y_l \wedge \mathbf{y}_{buf}^{(i)} < +s \right) \quad (3)$$

$$\mathbf{X}_{right}^{(i)} = \mathbf{X}_{buf}^{(i)} \left(\mathbf{y}_{buf}^{(i)} > -s \wedge \mathbf{y}_{buf}^{(i)} < y_r \right). \quad (4)$$

The parameter s denotes a certain overlap and is chosen to 0.3 m to guarantee, that the road center is represented in both point sets (see Figure 4). For $\mathbf{X}_{left}^{(i)}$ and $\mathbf{X}_{right}^{(i)}$ the cross fall and the rut depth are computed.

2.4.1 Estimation of the road cross fall

Because of the transformation of the points into the road axis coordinate system explained before, we can estimate the cross fall by fitting a 2D line into the points $\mathbf{X}_{left}^{(i)}$ and $\mathbf{X}_{right}^{(i)}$ within a least squares adjustment. Equation (5) shows the functional relationship of the 2D line for the left side of the road

$$m_{left}^{(i)} \cdot \mathbf{y}_{left}^{(i)} + b^{(i)} - \mathbf{z}_{left}^{(i)} = 0, \quad (5)$$

but please note, that the same equation can be used for the right part as well. The slope of the line $m^{(i)}$ equals the cross fall of the road surface.

2.4.2 Estimation of the rut depth

Figure 5 visualizes the steps for the determination of the rut depth. We use the residuals $\Delta\tilde{\mathbf{X}}$ (black dots) of the line adjustment, describing the surface of the cross profile without the inclination. The noise of the residuals impacts the detection of the supporting points, where the virtual 2 m rod touches the road surface and consequently the computed rut depth. Because of this, we need to smooth the signal from the residuals $\Delta\tilde{\mathbf{X}}$ to describe the road surface properly (yellow curve). There are two options investigated in this study. The first method uses a moving average filter of a length of 0.1 m. The second approach approximates a cubic spline with five interior knots into the residuals $\Delta\tilde{\mathbf{X}}$. Both methods

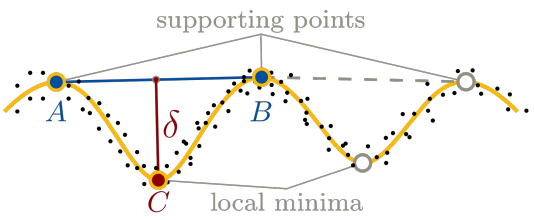

Figure 5. Scheme of the estimation of the rut depth

provide the smoothed points $\mathbf{X}_s$ on a regular grid with a width of 1 cm. They are then used to find local extrema representing the supporting points and the deepest location of the ruts. The number of ruts per lane is assumed to be two, so consequently we choose the two most prominent minima for the rut locations. If there are no minima detected, the rut depth is set to zero. The three most prominent maxima or saddle points are used as support points for the virtual 2 m rod, whereas the point in the center is used for both ruts. The rut depth $\delta^{(i)}$ is computed by the orthogonal distance between the virtual rod defined by the support points A and B and the minimum C (see Figure 5):

$$\delta^{(i)} = \frac{|(x_B - x_A)(y_C - y_A) - (y_B - y_A)(x_C - x_A)|}{\sqrt{(x_B - x_A)^2 + (y_B - y_A)^2}}. \quad (6)$$

Please note, that we compute $\delta_1^{(i)}$ and $\delta_2^{(i)}$ for each lane at every grid position $\mathbf{X}_{grid}^{(i)}$.

2.5 Evaluation of the uncertainty of the road quality parameters

For the evaluation, we use the multiple acquisitions of the road surface in both data sets. Reference data is unavailable for both data sets, so only the precision can be evaluated in this work. We compute the empirical standard deviation of the cross fall $s_m^{(i)}$ and of the rut depth $s_{\delta_1}^{(i)}, s_{\delta_2}^{(i)}$ for each grid point $\mathbf{X}_{grid}^{(i)}$ for both lanes separately. By analyzing the magnitude of these standard deviations for different grid point locations and data sets without changing the surface representation, we can derive the dependency of the environmental conditions on both parameters.

To evaluate the impact of the system calibration, the resulting parameters from the forward and backward passes are compared, since the impact of potential calibration errors on the point cloud data depends on the measuring configuration. Consequently, a constant difference between forward and backward passes should be present in case of a calibration error.

To evaluate the impact of the scanner properties on the parameter uncertainty, we modify the measured points $\mathbf{X}_{left}^{(i)}$ and $\mathbf{X}_{right}^{(i)}$ in two ways and re-estimate the parameters. To simulate a different sampling rate, we change the point spacing $\kappa_k = k \cdot \kappa_0$ (see section 2.3.1) by using only every k-th point in the point set. Furthermore, we add normal distributed noise σ_z to the z-component of the measured points,

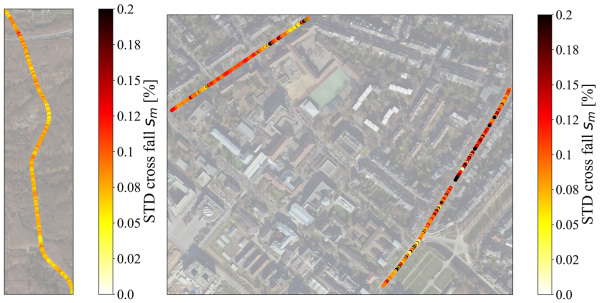

(a) Country road data set (b) Urban data set

Figure 6. Empirical standard deviation of the road cross fall for every grid point

to simulate higher noise in the range measurement. This procedure is done 1000 times for different point spacings κ and noise levels σ_z. We then compute the standard deviation $s_m^{(i)}$ and $s_\delta^{(i)}$ out of these estimations and compare them between the different simulated scanner properties.
To evaluate the impact of the surface representation on the rut depth, the simulation is performed for the two representation approaches explained in 2.4.2 and the results are compared.

3 Results

The cross fall changes between -8 % and 6 % in the country road data set and between -1 % and 5% in the urban data set. The mean rut depth is 5 mm for both data sets. We structure the results from our uncertainty evaluation based on the four questions from section 1.

3.1 Impact of environmental conditions

Figure 6 shows the standard deviation of the cross fall $s_m^{(i)}$ for both data sets along the investigated road parts for one lane. They do not differ depending on the location within one data set, but the average standard deviation is slightly higher in the campus data set. The shape of the cross section is curved and not linear in this data set, which negatively influences the cross fall estimation using the line adjustment. The same findings are made for the rut depth. That means, the environmental conditions have no significant influence on the road cross fall or the rut depth. Since the scanner is mounted, such that the scanning profile is perpendicular to the driving direction, the road cross section is captured within one scanning profile. Consequently, the uncertainty of the trajectory information does not influence the computation of the parameters except the roll angle of the vehicle for the cross fall. This orientation angle seems not to be influenced by the environmental conditions.

3.2 Impact of system calibration

Figure 7a shows the residuals of the cross fall $\mathbf{v}_m^{(i)}$ with respect to the mean value for each grid point location in the country road data set. The forward (FW) and backward (BW) passes are symbolized with upper and upside-down triangles colorized differently for each pass. We observe a systematic offset between all forward and backward passes of around 0.2%, which stays constant for all grid points and data sets. Larger residuals can be explained by occlusion due to traffic and remaining outlier points in the point cloud. The reason behind this is an error in the boresight angle of the system calibration, which causes a tilt of the point cloud across the driving direction.
By analyzing the rut depth residuals $\mathbf{v}_\delta^{(i)}$ for every grid point (see Figure 7b), no systematic offset between forward and backward passes are present, so no influence of the system calibration is visible. Since the rut depth is computed using the residuals from the line estimation, the systematic errors in the system calibration are canceled out. A variation of the other calibration parameters did not affect any of both parameters significantly.

3.3 Impact of scanner properties

For the evaluation of the impact of the scanner properties, we chose one grid point location for the analysis described in section 2.5. Figure 8a shows the empirical standard deviation of the road cross fall computed from the simulations for different scanner properties. We observe an increasing standard deviation by an increase of the sensor noise σ_z and the point spacing κ. Furthermore, we see that the noise level has a higher impact on the cross fall than the point spacing. If we only increase the noise level, the value of s_m also increases significantly, which does not count for the point spacing in this case. The standard deviation of the rut depth (see Figure 8b), however, increases depending on both properties the same way, since the shape of the heat map differs from the cross fall result.

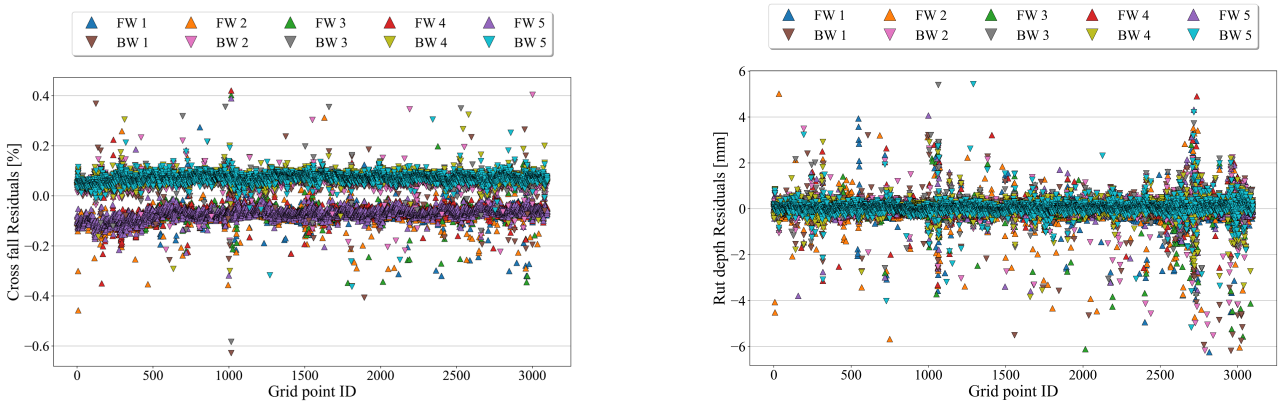

(a) Cross Fall residuals

(b) Rut depth residuals

Figure 7. Residuals of the road quality paraemters w.r.t. mean value for all forward (FW) and backward (BW) passes at all grid point locations in the country road data set.

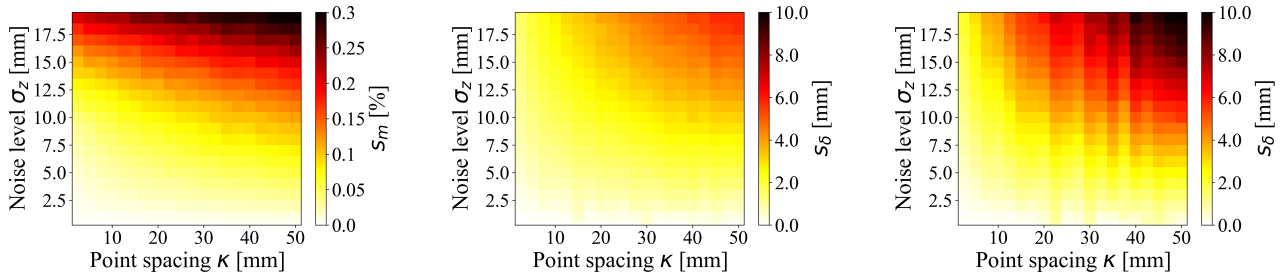

(a) Cross fall

(b) Rut depth spline smoothing

(c) Rut depth moving average smoothing

Figure 8. Standard deviations of the road quality parameters for different scanner properties and smoothing methods computed from simulation.

3.4 Impact of surface representation

For the evaluation of the impact of the surface representation, we compare the results from the spline smoothing (see Figure 8b) with the moving average solution (see Figure 8c). We observe, that the shape of the heat map does not change significantly between both figures. However, we see, that the magnitude of the s_δ differs significantly depending on the surface representation. The spline smoothing method provides more precise results than the moving average solution. Using this kind of simulation, other surface representations and rut depth estimations can be evaluated regarding their precision.

4 Conclusion

This paper presents a method to empirically evaluate the uncertainty of MMS in the context of the extraction of the road cross fall and the rut depth as two important road quality parameters. The approach analyzes the impact of four major influencing factors for the uncertainty of MMS point clouds in general: the trajectory information in different environmental conditions, the system calibration and the scanner properties. Furthermore, we analyzed the influence of the choice of the road surface representation on the rut depth estimation.

- The impact of the environmental conditions was analyzed considering two data sets with different GNSS conditions. At all locations along the road axis the standard deviation of both parameters stays constant and only varies because of the different shapes of the cross section of the road surface. This is due to the measuring configuration, which makes the instantaneous measurement of the cross section nearly independent from the GNSS quality.
- The impact of the system calibration on the un-

certainty of the road quality parameters was analyzed by comparing the derived parameters from different driving directions. For the cross fall a systematic offset between forward and backward passes for both data sets was detected. The most likely explanation would be an error in one boresight angle since the error stays constant. This does not count for the rut depth estimation, since there is no such systematic offset visible. This is due to the fact, that the rut depth estimation mainly relies on the surface representation of the road and not on its position or orientation.

- The impact of the scanner properties was analyzed by simulating different sensor noise and point densities. With increasing sensor noise and point spacing, the standard deviation of both parameters increases significantly.
- The impact of the surface representation on the uncertainty of the rut depth was analyzed by comparing the results of two approaches with different scanner properties. It can be seen, that the surface representation plays an important role, especially for data with a higher noise level and point spacings.

Additional reference information would enable the evaluation of the accuracy. The evaluation method can be performed on other road quality parameters, like longitudinal evenness. The impact of the influencing factors considered in this work may vary for these parameters, which can be analyzed with the presented approach.

References

Baffour, R. A. (2002). Collecting roadway cross slope data using multi-antenna-single receiver gps configuration. In *Applications of Advanced Technologies in Transportation (2002)*, pages 354–361.

FGSV (2009). Technische Prüfvorschriften für Ebenheitsmessungen auf Fahrbahnoberflächen in Längs- und Querrichtung (TP Eben), Teil: Berührungslose Messungen, 404/2. Technical report, Forschungsgesellschaft für das Straßen- und Verkehrswesen (FGSV).

Fwa, T. F., Pasindu, H. R., and Ong, G. P. (2012). Critical rut depth for pavement maintenance based on vehicle skidding and hydroplaning consideration. *Journal of Transportation Engineering*, 138(4):423–429.

Heinz, E., Holst, C., Kuhlmann, H., and Klingbeil, L. (2020). Design and Evaluation of a Permanently Installed Plane-Based Calibration Field for Mobile Laser Scanning Systems. *Remote Sensing*, 2020(12):555, doi:10.3390/s12030555.

Liu, R., Ren, H., Chai, Y., and Yang, J. (2022). 3d rutting features extraction through continuous pavement laser point cloud. *International Journal of Pavement Research and Technology*, 16:1–14.

Ma, X., Yue, D., Li, J., Wang, R., Yu, J., Liu, R., Zhou, M., and Wang, Y. (2024). Rutting extraction from vehicle-borne laser point clouds. *Automation in Construction*, 168:105853.

Miraliakbari, A., Hahn, M., and Maas, H.-G. (2014). Development of a multi-sensor system for road condition mapping. *The International Archives of the Photogrammetry, Remote Sensing and Spatial Information Sciences*, XL-1:265–272.

NovAtel Inc (2024). *Waypoint Inertial Explorer Post Processing Software*. URL: https://novatel.com/support/waypoint-software/inertial-explorer (last access: 23.04.2024).

Shams, A., Sarasua, W., Famili, A., Davis, W., and Mammadrahimli, A. (2018). Highway cross-slope measurement using mobile lidar. *Transportation Research Record: Journal of the Transportation Research Board*, 2672:036119811875637.

Teunissen, P. J. G. and Montenbruck, O., editors (2017). *Springer Handbook of Global Navigation Satellite Systems*, page 618. Springer International Publishing Switzerland.

Tsai, Y. J., Ai, C., Wang, Z., and Pitts, E. (2013). Mobile cross-slope measurement method using lidar technology. *Transportation Research Record*, 2367(1):53–59.

Zhou, Y., Wang, D., Xie, X., Ren, Y., Li, G., Deng, Y., and Wang, Z. (2014). A fast and accurate segmentation method for ordered lidar point cloud of large-scale scenes. *IEEE Geoscience and Remote Sensing Letters*, 11(11):1981–1985.

Zoller & Fröhlich GmbH (2020). Z+f profiler 9012, 2d laserscanner. Technical report, URL: https://www.zf-laser.com/Z-F-PROFILER-R-9012.2d_laserscanner.0.html (last access: 24.01.2020).